

Influence of harmonic voltage coupling on torque ripple of permanent magnet synchronous motor

SHENGTAO GENG, YONG ZHANG, HONGBO QIU, CUNXIANG YANG, RAN YI

Zhengzhou University of Light Industry, China
e-mail: zhangxiaoyong10056@163.com

(Received: 26.10.2018, revised: 28.01.2019)

Abstract: The permanent magnet synchronous motor (PMSM) driven by an inverter is widely used in the industrial field, but the inverter has a significant impact on the operational stability of the PMSM. The torque ripple of the PMSM is directly affected by the coupling of multiple harmonic voltages in the motor windings. In order to analyze its influence, a water-cooled PMSM with 20 kW 2000 r/min is taken as an example to establish the finite element model of the prototype, and the correctness of the model is verified by experiments. Firstly, based on the finite element method, the electromagnetic field of the PMSM is numerically solved in different operating states, and the performance parameters of the PMSM are obtained. Based on these parameters, the influence of the harmonic voltage amplitude on the torque ripple is studied, and the influence law is obtained. Secondly, combined with the decoupling analysis method, the influence of harmonic voltage coupling on the torque ripple is compared and analyzed, and the variation law of harmonic voltage coupling on the torque ripple is obtained. In addition, the influence of different harmonic voltage coupling on the average torque of the PMSM is studied, and the influence degree of different harmonic voltage amplitude on the torque fluctuation is determined. The conclusion of this paper provides reliable theoretical guidance for improving motor performance.

Key words: PMSM, harmonic voltage coupling, torque ripple, inverter

1. Introduction

A permanent magnet synchronous motor (PMSM) has been widely used in many industrial applications due to its advantageous features such as high efficiency, high power density, wide constant-power operating capability, high intermittent overload capability, and low acoustic noise [1–5]. In order to better control and start the PMSM, it is necessary to combine an inverter



© 2019. The Author(s). This is an open-access article distributed under the terms of the Creative Commons Attribution-NonCommercial-NoDerivatives License (CC BY-NC-ND 4.0, <https://creativecommons.org/licenses/by-nc-nd/4.0/>), which permits use, distribution, and reproduction in any medium, provided that the Article is properly cited, the use is non-commercial, and no modifications or adaptations are made.

with the PMSM, which also brings many adverse effects to the PMSM. The harmonic voltage generated by the inverter is an important factor that causes the torque ripple. The harmonic magnetic field generated by harmonic voltage will cause an unbalanced magnetic pull, and the operational stability of the PMSM will be affected to varying degrees. In addition, due to the skin effect, the harmonic voltage caused by the inverter will increase the loss of the PMSM [6]. Therefore, it is necessary to study the influence of harmonic voltage on the PMSM.

In recent years, many scholars have studied the influence of harmonic voltage on the torque ripple of the PMSM. In reference [7], a method for the compensation of the torque ripple that is caused by motor unidealities in sensorless the PMSM drives is proposed, and a torque ripple compensator is developed for suppressing the harmonics in the estimated electromagnetic torque. In reference [8], a new approach is introduced where a genetic algorithm is used as an optimization tool where the maximum value of the cogging torque is used as an objective function, and a proper mathematical presentation of the cogging torque for the analysis synchronous motor is developed. In reference [9], this paper improves the torque ripple model by considering magnetic saturation, and employs this model for the optimal current design to improve the performance of torque ripple minimization for IPMSMs under different load conditions. In reference [10], a method for electromagnetic torque ripple and copper losses reduction in a (non-sinusoidal or trapezoidal) SM-PMSM is presented, and the method is based on an extension of classical d_q transformation. In reference [11], the simple DTC method/switching table for the PMSM is proposed, to reduce flux and torque ripples as well as mechanical vibrations. The method can significantly reduce the flux, torque ripples, mechanical vibrations and improves the quality of a current waveform. However, many researches only analyze the methods of weakening the torque ripple from the angle of algorithm and simulation. Many studies do not quantitatively analyze the influence degree of the coupled harmonic voltage on the torque ripple.

Based on the above problems, a water-cooled PMSM is taken as an example and uses the two-dimensional electromagnetic field model to calculate the torque ripple under different working conditions. The influence law of harmonic voltage coupling on the torque ripple is obtained, and the influence degree of harmonic voltage coupling on the torque ripple is given. In addition, the influence of harmonic voltage coupling on the average torque is analyzed, and the variation law is also obtained. Some useful conclusions are obtained, which provide a basis for further study of the PMSM.

2. Motor parameters and models

2.1. Parameters and models

The research object of this paper is a water-cooled PMSM with 20 kW, 2000 r/min, focusing on the influence of harmonic voltage coupling on torque ripple of PMSM. Based on the actual structure of the prototype, the two-dimensional finite element model of the prototype is established, as shown in Fig. 1. In the finite element model, the total number of meshes is 27990, which can meet the accuracy of the solution. The winding structure and prototype are shown in Fig. 2, and the basic parameters are shown in Table 1.

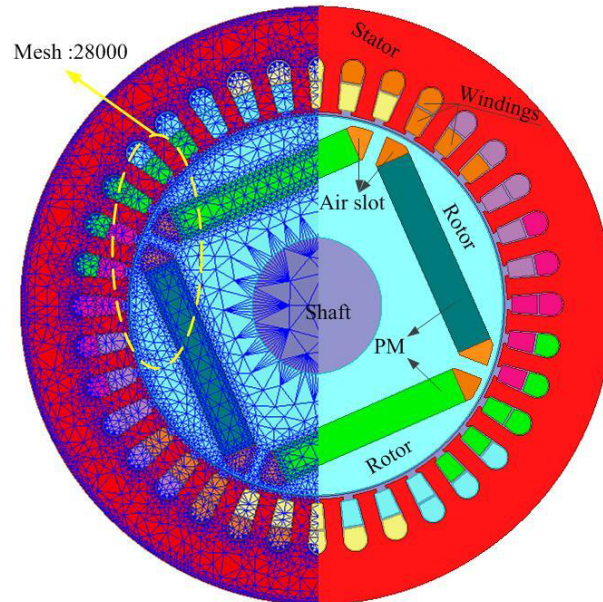


Fig. 1. Finite element model of prototype



Fig. 2. Winding structure and prototype of water-cooled PMSM

In the process of electromagnetic analysis of the prototype, the following assumptions are made to simplify the calculation [12]:

1. Ignore the leakage inductance at the end of the motor. It is assumed that the magnetic vector A has only the component in the z -axis direction.
2. Without considering the influence of the motor displacement current, the parallel plane field perpendicular to the motor shaft is adopted to analyze the electromagnetic field of the motor.
3. The conductivity and permeability of the material are constant ignoring the negligible influence of the temperature.

Table 1. Basic parameters of prototype

Parameters	Value	Unit
Rated power	20	kW
Rated speed	2000	r/min
Pole number	4	
Frequency	66.66	Hz
Axial length	90	mm
Rotor magnetic circuit structure	Interior type	
Stator outer diameter	210	mm
Stator inner diameter	136	mm
Slot number	36	
Number of parallel branches	1	
Winding connection type	Y	
Number of turns	20	

Based on the above assumptions, the two-dimensional electromagnetic field calculation formula is (1) [13, 14].

$$\left\{ \begin{array}{l} \Omega_1 : \frac{\partial}{\partial x} \left(\frac{1}{\mu} \frac{\partial A_z}{\partial x} \right) + \left(\frac{1}{\mu} \frac{\partial A_z}{\partial y} \right) = J_z + \sigma \frac{dA_z}{dt} \\ \Omega_2 : \text{curl} \left(\frac{1}{\mu} \text{curl} A_z \right) = \text{curl} M \\ \Gamma_1 : A_z = 0 \\ \Gamma_2 : \frac{1}{\mu_1} \frac{\partial A_z}{\partial n} - \frac{1}{\mu_2} \frac{\partial A_z}{\partial n} = J_s \end{array} \right. , \quad (1)$$

where: Ω_1 is the calculation region of an external permanent magnet, Ω_2 is the calculation region of an internal permanent magnet, A_z and J_z are the magnetic vector potential and the source current density in the z -axial component, respectively, J_s is the equivalent current density of permanent magnets, M is the magnetization vector within the permanent magnet area, n is the normal direction of permanent magnet boundary, σ is the conductivity, μ is the permeability, Γ_1 is the parallel boundary condition, Γ_2 is the PM boundary condition, μ_1 and μ_2 are the relative permeability, and t is time.

2.2. Experimental test and data comparison

In order to verify the accuracy of the model, the prototype is tested with the use of an experimental platform. The experimental platform includes an EMC900 dynamometer machine, HIOKI PW6001 power analyzer, industrial condensing unit, DSP data acquisition system and

other experimental equipment. The experimental platform of the prototype is shown in Fig. 3. Under different operating conditions, the experimental data of torque, no-load back EMF and current are obtained. The experimental data are compared with the calculated data, as shown in Table 2.



Fig. 3. Test platform of prototype

Table 2. Comparison of the test data and the finite element model calculated results

Power	Comparison Parameter	Test data	Calculated results	Variation rate
10 kW	Current (A)	19.8	19.1	3.5%
	Average torque (N · m)	47.4	46.8	1.3%
15 kW	Current (A)	28.3	27.4	3.2%
	Average torque (N · m)	69.5	70.6	1.6%
20 kW	Current (A)	36.4	35.9	1.1%
	Average torque (N · m)	97.5	96.4	1.1%
No-load back EMF (V)		315	324	2.8%

It can be seen from Table 2 that the errors are within 5%. The calculated results are in good agreement with the experimental data under different powers, which verifies the accuracy of the finite model.

3. Harmonic voltage analysis of PMSM

When PMSM is driven by inverter, the power supply of the input motor is non-sinusoidal, and a lot of harmonic components are contained in the voltage source. The input voltage is decomposed by Fourier decomposition, and a series of sine waves are decomposed. The mathematical expression of the three-phase coupled voltage harmonic is Eq. (2) [15].

$$\begin{cases} U_A = \sum_{\mu=1,2,\dots}^{\infty} \sqrt{2U_{\mu}} \cos [\mu(\omega t + \varphi_{\mu})] \\ U_B = \sum_{\mu=1,2,\dots}^{\infty} \sqrt{2U_{\mu}} \cos [\mu(\omega t - 120) + \varphi_{\mu}] \\ U_C = \sum_{\mu=1,2,\dots}^{\infty} \sqrt{2U_{\mu}} \cos [\mu(\omega t + 120) + \varphi_{\mu}] \end{cases}, \quad (2)$$

where: U_{μ} is the effective value of the μ -th harmonic voltage, μ is the harmonic order, φ_{μ} is the initial phase angle of the μ -th harmonic voltage.

The stator winding of the PMSM is connected by Y , and the harmonic component of $\mu = (3n)$ th does not exist in the motor winding. The rotation speed of the $\mu = (6n - 1)$ th time harmonic magnetic field is μ times of the fundamental synchronous speed, and the rotation direction is opposite to the rotation direction of the fundamental magnetic field. The rotation speed of the $\mu = (6n+)$ th time harmonic magnetic field is μ times of the fundamental synchronous speed, and the rotation direction is the same as the rotation direction of the fundamental magnetic field. n is a positive integer.

To sum up, the magnetomotive force generated by the time harmonic voltage rotates at a high speed relative to the fundamental magnetomotive force, which is bound to have an impact on the torque ripple of the motor. In general, the 5th, 7th, 11th, and 13th harmonic contents are relatively large, which has a serious impact on the torque ripple of the PMSM [16, 17]. Therefore, the above harmonic voltage orders are selected to study the influence of harmonic voltage coupling on torque ripple of a PMSM.

4. Influence of harmonic voltage coupling on torque ripple of PMSM

The torque ripple of PMSM limits its application in high-precision situations, especially in low-speed driving situations, and also leads to vibration and noise of the motor [18]. Among the factors affecting the torque ripple of the PMSM, a higher harmonic of voltage is the key factor. The fundamental voltage and harmonic voltage form their respective rotating magnetic fields in the air gap. The electromagnetic torque produced by fundamental voltage and harmonic voltage is stable, but the coupled magnetic field caused by the interaction of two magnetic fields is unstable, and has pulsating properties, thus forming the torque ripple [19, 20].

$$T_{\text{ripple}} = \left| \frac{T_{\text{max}} - T_{\text{min}}}{2T_{\text{avg}}} \right|, \quad (3)$$

where: T_{ripple} is the torque ripple, T_{max} is the maximum value of torque in a cycle, T_{min} is the minimum value of torque in a cycle and T_{avg} is the average value of torque in a cycle.

Based on the finite element method, the following is analyzed:

1. The influence of harmonic voltage content on the torque ripple of a PMSM is analyzed.
2. The variation of the torque ripple of the PMSM is analyzed when different harmonic voltages are coupled with each other. In addition, in order to compare and analyze, the influence of a single harmonic voltage on the torque ripple is analyzed.
3. The influence of harmonic voltage coupling on the average torque of the PMSM is analyzed.

4.1. Influence of harmonic voltage content on torque ripple of PMSM

Based on the finite element method, the fundamental voltage is contained in an armature winding of a PMSM. The harmonic voltage of 5th, 7th, 11th and 5th + 7th + 11th with different amplitudes is selected as an example, and the variation of the torque ripple of the PMSM is obtained, as shown in Fig. 4.

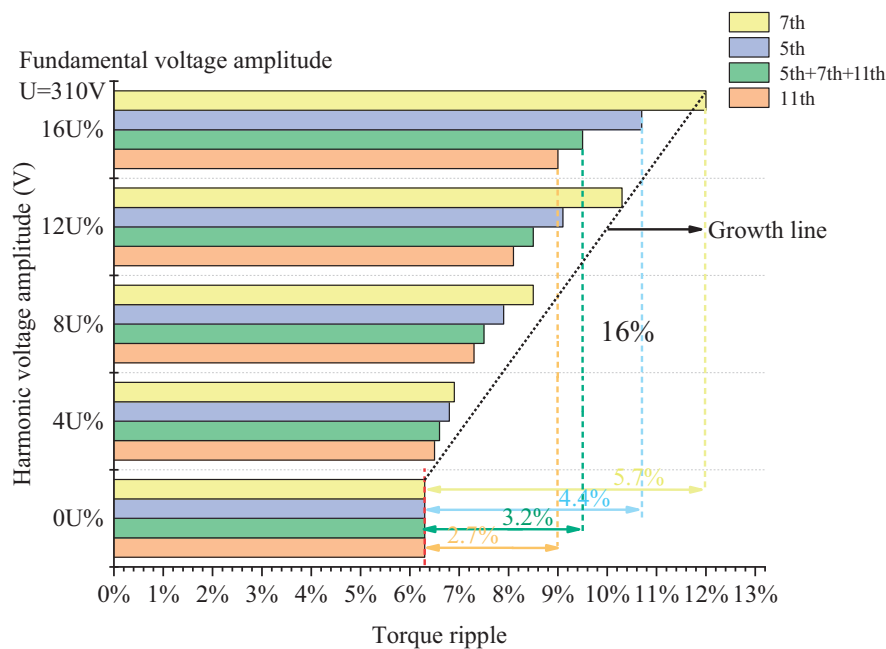


Fig. 4. The variation of torque ripple with amplitude

It can be seen from Fig. 4 that when the higher harmonics is contained in voltage source, the torque ripple increases sharply, and the torque ripple increases linearly with the increase of the harmonic voltage amplitude.

The torque ripple is 6% when only the fundamental voltage is contained in the motor winding. When the harmonic voltage amplitude of 5th, 7th, 11th and 5th + 7th + 11th increases to 16% of the fundamental voltage, the torque ripple increases by 4.4%, 5.7%, 2.7% and 3.2% respectively.

When the harmonic voltage amplitude increases by 16% of the fundamental voltage, the torque ripple of 5th, 7th, 11th, 5th + 7th + 11th are 1~2 times of the torque ripple when only the fundamental voltage is contained. When the harmonic voltage amplitude is the same, the 5th and 7th harmonic voltages have a great influence on the torque ripple. It can be seen that the higher harmonics of the voltage have a great influence on the operational stability of the PMSM. In practical applications, it is necessary to reduce the harmonic content of the inverter input PMSM by effective means, improve the operational stability of the PMSM, and reduce the noise and vibration of the PMSM.

4.2. Influence of harmonic voltage coupling on torque ripple

When the PMSM is driven by the inverter, the harmonic orders of winding are not single, but multiple harmonic voltages are coupled with each other. The coupling of higher harmonics with different rotating directions and rotating speeds will have an important impact on the torque ripple of the PMSM. The torque ripple is analyzed when the 5th, 7th, 11th and 13th harmonic voltages exist separately. When the 5th, 7th, 11th and 13th harmonic voltages are coupled to each other, the torque ripple is also analyzed. The variation of the torque ripple is shown in Fig. 5.

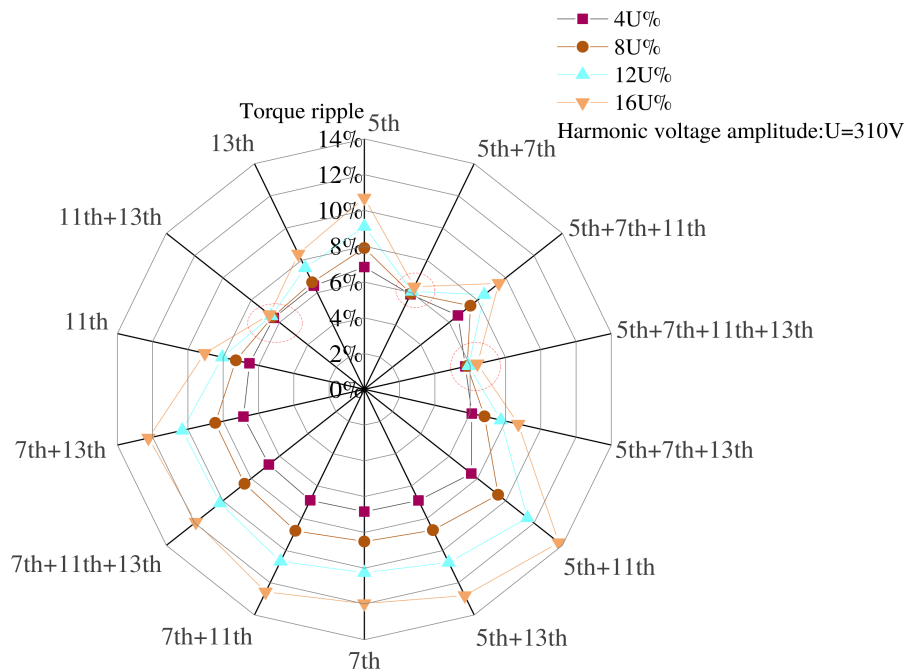


Fig. 5. Torque ripple of harmonic coupling

It can be seen from Fig. 5 that when the multiple harmonic voltage are coupled to each other, the torque ripple changes significantly. The torque ripple of 5th + 7th, 11th + 13th, 5th + 7th + 11th + 13th is significantly smaller than that of the interaction of the fundamental and a single harmonic. The torque ripple is the smallest when 5th + 7th + 11th + 13th is coupled,

concentrating around 6%. Compared with the influence of the single harmonic on the torque ripple, the influence of the 5th + 7th, 11th + 13th, 5th + 7th + 11th + 13th on the torque ripple shows a negative synergistic effect.

The torque ripple of 7th + 13th, 7th + 11th, 7th + 11th + 13th, 5th + 13th, 5th + 11th, 5th + 7th + 13th, 5th + 7th + 11th is greater than that of the interaction of the fundamental and a single harmonic. The torque ripple is the largest under the same voltage harmonic amplitude, when 5th + 11th is coupled, showing a positive synergistic effect. It can be seen that the torque ripple caused by the coupling of the fundamental and multiple harmonic voltages can be lower than the torque ripple of the fundamental and a single harmonic. Therefore, based on the negative synergy effect, when the PMSM is driven by the inverter, some effective means such as the harmonic injection method is used to add a certain harmonic order in the motor winding to reduce the torque ripple.

4.3. Influence of harmonic voltage coupling on average torque

Considering that the average torque of the PMSM directly determines the ability of the motor to drag the load, the variation of the average torque is analyzed when the harmonic voltage is coupled with each other. When the different harmonic voltage orders are coupled in the stator winding, the influence of harmonic voltage coupling on the average torque of the motor is analyzed, as shown in Table 3.

Table 3. The variation of average torque

Coupling of different harmonic voltage orders	Average torque with different harmonic voltage amplitudes (N·m)					Maximum increment
	0%	4%	8%	12%	16%	
5	96.40	96.41	96.44	96.47	96.50	0.1
5 + 7	96.40	96.41	96.43	96.46	96.49	0.09
5 + 7 + 11	96.40	96.42	96.44	96.48	96.52	0.12
5 + 7 + 11 + 13	96.40	96.42	96.44	96.48	96.52	0.12
5 + 7 + 13	96.40	96.42	96.45	96.48	96.52	0.12
5 + 11	96.40	96.41	96.44	96.48	96.52	0.12
5 + 13	96.40	96.42	96.44	96.48	96.53	0.13
7	96.40	96.40	96.42	96.44	96.48	0.08
7 + 11	96.40	96.41	96.42	96.45	96.49	0.09
7 + 11 + 13	96.40	96.40	96.42	96.45	96.49	0.09
7 + 13	96.40	96.41	96.43	96.46	96.51	0.11
11	96.40	96.40	96.40	96.41	96.41	0.01
11 + 13	96.40	96.40	96.40	96.41	96.41	0.01
13	96.40	96.40	96.41	96.42	96.43	0.03

As can be seen from Table 3, with the increase of harmonic voltage amplitude, the average torque of the motor is not significantly affected. In addition, the influences of the multiple harmonic voltages coupling on the average torque are also very small. With the increase of harmonic voltage amplitude, the average torque also gradually increases. The maximum increment of the average torque appears at 5th + 13th, which is $0.13 \text{ N} \cdot \text{m}$. The maximum variation range of the average torque only is 0.13%.

5. Conclusions

In this paper, a 2000 r/min 20 kW PMSM is taken as an example. Based on the finite element method, the influences of multiple harmonic voltages coupling on the average torque and torque ripple of the PMSM are analyzed, and the following conclusions are obtained:

1) The existence of harmonic voltage can cause a large torque ripple, and the torque ripple increases linearly with the amplitude of harmonic voltage. When only the fundamental voltage is contained in the motor windings, the torque ripple is 6%. When the harmonic voltage amplitudes of 5th, 7th, 11th, and 5th + 7th + 11th increases to 16% of the fundamental voltage, the torque ripple increases by 4.4%, 5.7%, 2.7%, and 3.2% respectively. Compared with the torque ripple of fundamental voltage, the torque ripple is increased by 1–2 times. At the same harmonic voltage amplitude, the 5th and 7th harmonic voltages have a great influence on the torque ripple. In practical applications, the inverter output harmonic content should be reduced by effective means to improve the running stability of the motor and reduce the noise and vibration of the motor.

2) The coupling of higher harmonic voltages can effectively reduce the torque ripple. The difference between the torque ripple of 5th + 7th + 11th + 13th and the torque ripple of fundamental voltage is small, both around 6%. Therefore, based on the negative synergy effect, when the PMSM is driven by the inverter, some effective means such as the harmonic injection method is used to add a certain harmonic order in the motor winding to reduce the torque ripple.

3) When different harmonic voltages are coupled to each other in the stator windings, the average torque of the PMSM is a slight change. The maximum increment of the average torque appears at 5th + 13th, which is $0.13 \text{ N} \cdot \text{m}$. The maximum fluctuation range of the average torque only is 0.13%. Therefore, in the application of the PMSM driven by an inverter, the influence of harmonic voltage on the average torque should not be considered too much.

Acknowledgements

This work was supported in part by the National Natural Science Foundation of China under Grant 51507156, in part by the University Key Scientific Research Programs of Henan province under Grant 17A470005, in part by the Key R&D and Promotion Projects of Henan Province under Grant 182102310033, in part by the Doctoral Program of Zhengzhou University of Light Industry under Grant 2014BSJJ042, and in part by the Foundation for Key Teacher of Zhengzhou University of Light Industry.

References

- [1] Zhu G., Zhu Y., Tong W., Han X., Zhu J., *Double-Circulatory Thermal Analyses of a Water-Cooled Permanent Magnet Motor Based on a Modified Model*, IEEE Transactions on Magnetics, vol. 54, no. 3, pp. 1–4 (2018).

- [2] Zhang B., Qu R., Wang J., Xu W., Fan X., Chen Y., *Thermal Model of Totally Enclosed Water-Cooled Permanent-Magnet Synchronous Machines for Electric Vehicle Application*, IEEE Transactions on Industry Applications, vol. 51, no. 4, pp. 3020–3029 (2015).
- [3] Su Y.X., Zheng C.H., Duan B.Y., *Automatic disturbances rejection controller for precise motion control of permanent-magnet synchronous motors*, IEEE Transactions on Industrial Electronics, vol. 52, no. 3, pp. 814–823 (2005).
- [4] Choi H.H., Vu N.T., Jung J., *Digital Implementation of an Adaptive Speed Regulator for a PMSM*, IEEE Transactions on Power Electronics, vol. 26, no. 1, pp. 3–8 (2011).
- [5] Nowak L., Knypinski L., Jedryczka C., Kowalski K., *Decomposition of the compromise objective function in the permanent magnet synchronous motor optimization*, Compel – The International Journal For Computation And Mathematics In Electrical And Electronic Engineering, vol. 34, pp. 496–504 (2015).
- [6] Hemeida A., Sergeant P., Vansompel H., *Comparison of Methods for Permanent Magnet Eddy-Current Loss Computations with and without Reaction Field Considerations in Axial Flux PMSM*, IEEE Transactions on Magnetics, vol. 51, no. 9, pp. 1–11 (2015).
- [7] Piippo A., Luomi J., *Torque Ripple Reduction in Sensorless PMSM Drives*, IECON 2006 – 32nd Annual Conference on IEEE Industrial Electronics, Paris, pp. 920–925 (2006).
- [8] Cvetkovski G., Petkovska L., *Cogging torque minimisation of PM synchronous motor using genetic algorithm*, International Journal of Applied Electromagnetics and Mechanics, vol. 46, pp. 327–334 (2014).
- [9] Lai C., Feng G., Mukherjee K., Loukanov V., Kar N.C., *Torque Ripple Modeling and Minimization for Interior PMSM Considering Magnetic Saturation*, IEEE Transactions on Power Electronics, vol. 33, no. 3, pp. 2417–2429 (2018).
- [10] Oliveira A.A., Aguiar M.L. Jr, Sanagiotti E.R., *Electromagnetic torque ripple and copper losses reduction in permanent magnet synchronous machines*, European Transactions on Electrical Power, vol. 22, no. 5, pp. 627–644 (2012).
- [11] Sivaprakasam A., Manigandan T., *A simple method to reduce torque ripple and mechanical vibration in direct torque controlled permanent magnet synchronous motor*, Journal of Vibroengineering, vol. 15, no. 2, pp. 658–674 (2013).
- [12] Weili L., Xiaochen Z., Baoquan K., *Loss calculation and thermal simulation analysis of high-speed PM synchronous generators with rotor topology*, 2010 International Conference on Computer Application and System Modeling (ICCA SM 2010), Taiyuan, pp. V14-612-V14-616 (2010).
- [13] Li W., Zhang X., Cheng S., Cao J., *Thermal Optimization for a HSPMG Used for Distributed Generation Systems*, IEEE Transactions on Industrial Electronics, vol. 60, no. 2, pp. 474–482 (2013).
- [14] Kowalski K., Nowak L., Knypinski L., Idziak P., *Influence of the core saturation on the dynamic performance of the magnetostrictive actuator*, Archives Of Electrical Engineering, vol. 66, pp. 523–531 (2017).
- [15] Yamazaki K., Abe A., *Loss Investigation of Interior Permanent-Magnet Motors Considering Carrier Harmonics and Magnet Eddy Currents*, IEEE Transactions on Industry Applications, vol. 45, no. 2, pp. 659–665 (2009).
- [16] Chunting Mi, Filippa M., Weiguo Liu, Ruiqing Ma, *Analytical method for predicting the air-gap flux of interior-type permanent-magnet machines*, IEEE Transactions on Magnetics, vol. 40, no. 1, pp. 50–58 (2004).
- [17] Binns K.J., Jabbar M.A., *High-field self-starting permanent-magnet synchronous motor*, IEE Proceedings B – Electric Power Applications, vol. 128, no. 3, pp. 157–160 (1981).

- [18] Ou L., Wang X., Xiong F., Ye C., *Reduction of torque ripple in a wound-rotor brushless doubly-fed machine by using the tooth notching*, IET Electric Power Applications, vol. 12, no. 5, pp. 635–642 (2018).
- [19] Kermanipour M.J., Ganji B., *Modification in Geometric Structure of Double-Sided Axial Flux Switched Reluctance Motor for Mitigating Torque Ripple*, Canadian Journal of Electrical and Computer Engineering, vol. 38, no. 4, pp. 318–322 (2015).
- [20] Knypinski L., Nowak L., *Optimization of the permanent magnet brushless DC motor employing finite element method*, Compel – The International Journal For Computation And Mathematics In Electrical And Electronic Engineering, vol. 32, pp. 1189–1202 (2013).